

pubs.acs.org/NanoLett Letter

# **Optically Gated Electrostatic Field-Effect Thermal Transistor**

Shouyuan Huang, Neil Ghosh, Chang Niu, Yong P. Chen, Peide D. Ye, and Xianfan Xu\*



Cite This: https://doi.org/10.1021/acs.nanolett.3c05085



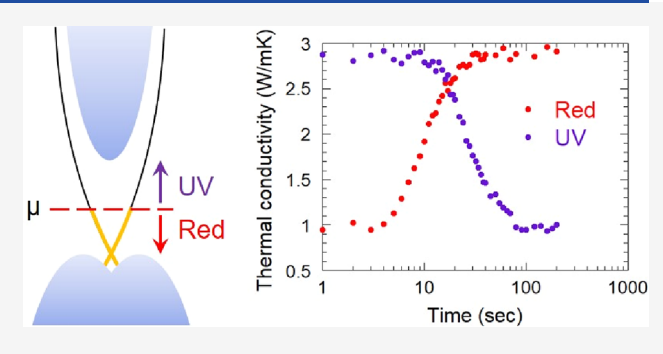
**ACCESS** 

Metrics & More

Article Recommendations

Supporting Information

ABSTRACT: Dynamic tuning of thermal transport in solids is scientifically intriguing with wide applications for thermal transport control in electronic devices. In this work, we demonstrate a thermal transistor, a device in which heat flow can be regulated using external control, realized in a topological insulator (TI) through the topological surface states. The tuning of thermal transport is achieved by using optical gating of a thin dielectric layer deposited on the TI film. The gate-dependent thermal conductivity is measured using micro-Raman thermometry. The transistor has a large ON/OFF ratio of 2.8 at room temperature and can be continuously and repetitively switched in tens of seconds by optical gating and potentially much faster by electrical gating. Such thermal



transistors with a large ON/OFF ratio and fast switching times offer the possibilities of smart thermal devices for active thermal management and control in future electronic systems.

KEYWORDS: thermal transistor, thermal switch, electrostatic gating, topological insulator

hermal transistors are devices capable of turning heat transfer on and off using an external control. 1-4 There are various approaches for switching thermal transport, for example, by bringing mechanical parts in and out of contact, which can be considered as an analog of a mechanical relay for electrical switching,<sup>5,6</sup> pumping thermally conductive fluid in and out of the thermal transport channel, 6,7 utilizing metalinsulator or liquid-metal transitions caused by temperature change, 8-12 electrical control of molecular junctions, 13 electrochemical intercalation, 4,14-16 altering materials' structures by phase transitions <sup>17,18</sup> or pressure, <sup>19</sup> and radiation, <sup>12</sup> especially in the near-field by changing the coupling between surface phonon polaritons.<sup>20</sup> It is desirable to realize thermal transistors on the targeted material itself, with no moving parts and no alteration to its composition, while operating at a fixed temperature in addition to the essential features of a large ON/OFF ratio and a fast switching speed. However, very few effective solid-state thermal transistors with these features have been realized. For example, large ON/OFF ratios in thermal switching are usually obtained with a variable switching temperature, <sup>17</sup> long switching time due to the use of moving parts,<sup>5</sup> or the change of materials' structures.<sup>8,11,12</sup> A possible solution that does not involve moving parts or other mechanical means is the use of an external electric or magnetic field. It was demonstrated that thermal conductivity can be changed by altering the interface of thin films by an external electric field, 21 by altering phonon scattering via phase transformation using an external electric field, 22 or by phase transformation using electrolyte gating. 18 The thermal conductance of a molecular junction was tuned by 1300%

using an electric field with high switching speeds and repeatability, although with much-involved sample preparation. <sup>13</sup> Electronic thermal conductivity (i.e., not total thermal conductivity) in a ferromagnetic—nonmagnetic thin film stack was changed by about 20%<sup>23,24</sup> and up to 50% using a magnetic field. <sup>25</sup> Tuning thermal conductivity by changing bulk material structures using external fields has also been demonstrated; <sup>26–28</sup> however, these processes are usually not fast.

Switching thermal conduction by controlling the electronic carrier density and, thus, the electronic contribution to thermal transport can be a fast process. In some materials, the electronic carrier density can be electrically gate-tuned by orders of magnitude within a time duration far below one second.<sup>29</sup> However, gate-tuning of electronic thermal conductivity is also challenging because, in semiconductors, electrons only contribute to a few percent of the total thermal conductivity,<sup>30</sup> while the rest is due to phonon transport.<sup>31</sup> In metals, where electronic thermal conductivity dominates, a colossal voltage is required to change the electron density due to electrical screening.<sup>32</sup>

Here, we report a thermal transistor with a large ON/OFF ratio that can be tuned in tens of seconds by using optical

Received: December 23, 2023
Revised: April 15, 2024
Accepted: April 16, 2024



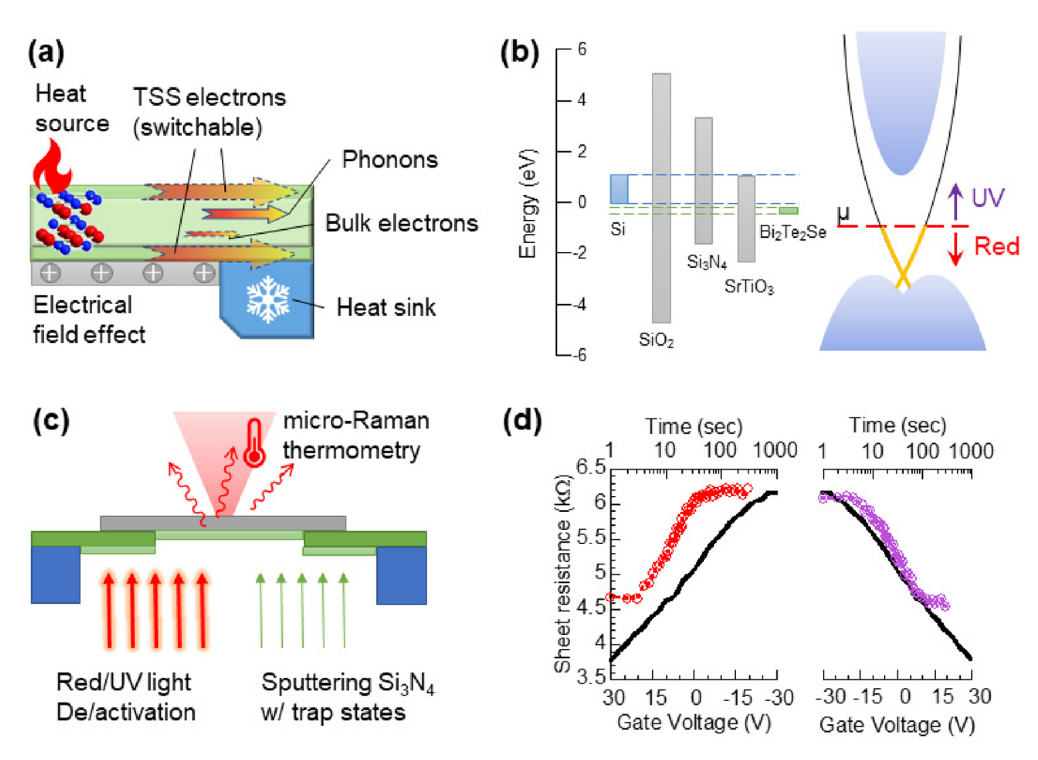


Figure 1. Optical gating for thermal switching and measurement. (a) Schematic of an electrical field-effect thermal transistor based on switching of TSS electrons in TI, whose ON/OFF states thermal conductivity are to be measured when the film is suspended. (b) Schematics of band structures with chemical potential tuning using optical illumination. (c) Schematics of the sputtering coating process of  $Si_3N_4$ , optical switching, and micro-Raman measurements of thermal transport. (d) Dark current of a 16 nm  $Bi_2Te_2Se$  transistor with  $Si_3N_4$  coating under red (red dots) and UV (purple dots) light illumination, compared with electrical gating (black lines), measured at -148 °C.

gating of a thin dielectric film deposited on a topological insulator (TI). Such transistors can be realized without lithography or chemical processing and modulated in realtime in a noncontact manner, offering an alternative to electrically gated devices. Topological insulators are emerging as a promising platform for novel quantum devices, 33,34 including alternative transistors due to their semiconducting bulk, unique spin texture of their surface states<sup>37</sup> (different from Weyl semimetals and Rashba systems), 40-42 spin-momentum locking, and backscattering protection. 43,44 Recent thermal transport studies on TI films offer a unique opportunity to develop an efficient thermal transistor.<sup>45</sup> For typical semiconductors or metals, the ratio of the electronic contribution of the thermal conductivity to the electrical conductivity, the Lorenz number, is approximately a constant, which is the Sommerfeld value,  $1.5-2.2 \times 10^{-8} \text{ V}^2/\text{K}^2$ . However, in a topological insulator, its topological surface state (TSS) electrons can possess a large Lorenz number, exceeding ten times the Sommerfeld value. 45 This large Lorenz number is a result of the chemical potential being near the Dirac point that results in the difference in energy and momentum scattering in TSS electrons, similar to that in graphene, <sup>46</sup> or by bipolar diffusion, or the combination of both. The large Lorenz number makes the gate-tuned thermal transport in TI possible, as changes in the electrical transport will be amplified in thermal transport. Moreover, in very thin TI films (e.g., Bi<sub>2</sub>Te<sub>2</sub>Se films less than 20 nm thick), thermal transport is dominated by TSS electrons.<sup>45</sup> For a typical semiconductor, the electrical field effect affects tens of nanometers into conductive solids due to electrical screening. Hence, for very thin TI films, the electrical field effect is sufficient to affect the charge density over the entire thickness of the film. In this

work, we explore and demonstrate large switching of heat transport in Bi<sub>2</sub>Te<sub>2</sub>Se thin films using the electrostatic effect.

Electrical gate tuning of thermal transport in TI is illustrated in Figure 1a, in which the heat conduction channel in TSS is switchable, i.e., turned on and off when the chemical potential is tuned by the electrical field effect via a back gate. Figure 1a also illustrates that in order to measure thermal transport along the in-plane direction of the thin film to demonstrate the tuning of thermal transport by the electrical field, it is preferable to suspend thin films so that the contribution to thermal transport by the substrate is removed to preserve the sensitivity of the thermal conductivity measurement (only half of the film is shown). However, the back gate electrode and the required insulating layer between the electrode and the thin film will also contribute significantly to thermal transport, much greater than the TI film, and hence will introduce a large uncertainty to the thermal transport measurement. An alternative is to use a vacuum gap as an insulator. However, such a gap is not effective in gating TSS, which is described in Supplementary Note 1, in addition to the many processes involved in sample preparation.

In this work, we employed an optical gating strategy to apply an electrical field to a thin TI film. The persistent and bidirectional nature of optical gating using red/UV light illumination has been demonstrated previously and used to fabricate photoconductive devices, 47,48 switch superconductivity in heterostructures, 49 and to pattern p-n junctions on topological insulator 50 or transition-metal dichalcogenide (TMD) 11 channels. These studies utilized the trap states generated by the intrinsic defects of either a deposited layer on the target device or the substrate on which it was fabricated. In this work, we chose a very thin silicon nitride (Si<sub>3</sub>N<sub>4</sub>) film (a

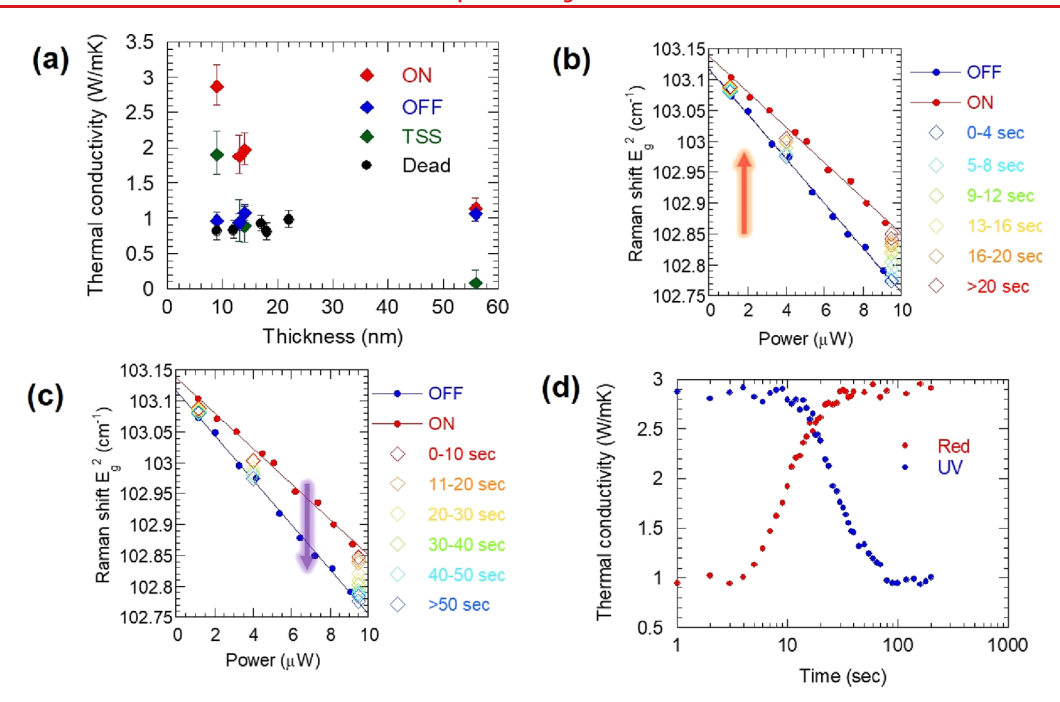


Figure 2. Optically gated Bi<sub>2</sub>Te<sub>2</sub>Se thermal transistor. (a) Thickness-dependent thermal conductivity at the ON/OFF states of Bi<sub>2</sub>Te<sub>2</sub>Se thin films. An ON/OFF ratio as large as 2.8 was obtained. The TSS contribution to thermal transport, obtained by subtracting the thermal conductivity at the OFF state from that at the ON state, along with the results of a few dead devices are also included. (b, c) Raman shift vs illumination power for the 9 nm film under red and UV illumination. Solid dots and linear fitting lines are the results from Raman measurements at nine different power levels after long illumination; diamonds are from three different power levels after each train of pulsed illumination using the red diode (b) and UV diode (c), indicated by red and violet arrow, with controlled exposure dosage. (d) Time history of thermal conductivity under red and UV illumination.

few nanometers thick) as it can be readily deposited on the TI film without affecting the thermal measurements significantly. The band alignments of Bi<sub>2</sub>Te<sub>2</sub>Se, Si<sub>3</sub>N<sub>4</sub>, and several other insulating films<sup>52</sup> along with the activation and deactivation processes during optical gating are illustrated in Figure 1b. A detailed explanation of the proposed optical gating mechanism is provided in Supplementary Note 2. The thin sputtered layer of Si<sub>3</sub>N<sub>4</sub> is used as an optical gate during the micro-Raman thermal transport measurement, as shown in Figure 1c.

To examine the effectiveness of optical gating and compare it with electrical back gating, thin film Bi<sub>2</sub>Te<sub>2</sub>Se transistors were fabricated on a SiO<sub>2</sub>/Si substrate. A 3 nm thick Si<sub>3</sub>N<sub>4</sub> layer was then sputtered on top of the Bi<sub>2</sub>Te<sub>2</sub>Se devices. Details of sample preparation are provided in Supplementary Note 3. The dark current of the device (without back gating) was measured after red and UV light exposure and then compared to the results obtained by using electrical back gating. The transfer curve  $(I_d-V_g)$  obtained from electrical back gating immediately after red light exposure is shown as black lines in Figure 1d in terms of sheet resistance, indicating that the chemical potential can be effectively moved toward/ away from the conduction band/charge neutral point and vice versa. These measurements were performed at a temperature of -148 °C, so the large increase and decrease in sheet resistances facilitate the comparison between the results from back gating and optical illumination. The time span in Figure 1d is for the optical measurements. It can be seen that the red light illumination charges the Si<sub>3</sub>N<sub>4</sub> thin film, leading to a negative gating effect, which increases the sheet resistance of the device and moves the chemical potential toward the charge neutral point. The inverse process occurs under UV light illumination; the Si<sub>3</sub>N<sub>4</sub> film becomes depopulated, effectively applying a positive back gate to the device, decreasing its sheet

resistance and moving chemical potential toward the conduction band. To further confirm the tuning of the chemical potential due to optical gating, Hall effect measurements were performed on the devices to obtain the 2D carrier concentrations after long red/UV light illumination cycles, and the results are presented in Supplementary Note 4. Therefore, these two optical transitions effectively move the chemical potential and switch thermal transport between the ON and OFF states, equivalent to electrical gating. However, as discussed previously, only optical gating was used in this work for the thermal transport measurement on the suspended films.

The thermal transport in Bi<sub>2</sub>Te<sub>2</sub>Se under optical gating was measured using micro-Raman thermometry (adapted from our previous work),<sup>53</sup> which has been widely used for measuring in-plane thermal transport in low-dimensional materials.<sup>53–62</sup> A detailed description of the thermal model used for extracting thermal conductivity and the uncertainty analysis is provided in Supplementary Note 5. The switching effect of the Raman laser beam itself on the thermal conductivity measurement is discussed in Supplementary Note 6.

Figure 2a summarizes the results of the thermal conductivity measurements on the thin  $\mathrm{Bi_2Te_2Se}$  films. Our earlier work indicated that for films with thicknesses less than ~20 nm, electrons in TSS dominate thermal transport. To demonstrate a large ON/OFF ratio of thermal transport due to the optical gating of TSS electrons, we focused on films below 20 nm, and a 56 nm thick sample is shown as a reference. Switching of thermal conductivity upon the red and UV light illumination was successfully demonstrated in samples with thicknesses of 9, 13, and 14 nm, as shown in Figure 2a. These samples were fabricated on different substrates; therefore, each one was not affected by red/UV illumination cycles of the

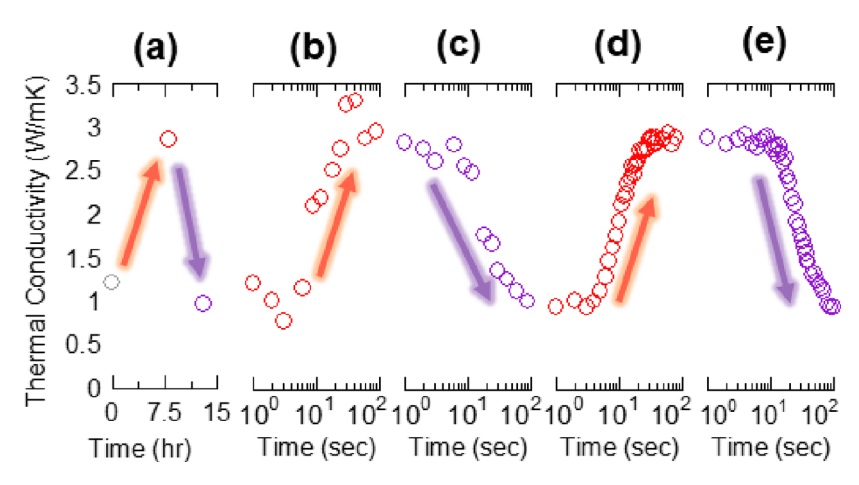


Figure 3. ON/OFF cycling of the thermal transistor. (a) First cycle under long illumination; (b-e) second and third cycles under pulsed illumination.

other samples. The ON and OFF state thermal conductivities shown in Figure 2a are from the long illumination cycles (a few hours) to find the largest ON/OFF ratio.

An ON/OFF ratio of 2.8 is obtained for the 9 nm sample, demonstrating the thermal transistor effect. The ON/OFF ratio of the other two films with slightly larger thicknesses is also greater than 2. For comparison, the 56 nm film showed just a slight variation of the thermal conductivity upon optical gating. Note that the high thermal conductivity of thinner films and the trend of the increase of thermal conductivity with the decrease of film thickness for the ON state is consistent with our previous results due to the larger contribution of TSS to thermal transport for thinner films. 45 These results indicate that we are indeed tuning the TSS contribution to thermal conductivity, also confirming that the large thin film thermal conductivity and large Lorenz number originate from the TSS electrons. To further corroborate our results, we also compared the obtained thermal conductivity data against predictions made by a two-layer transport model adapted from our previous work.<sup>63</sup> A detailed discussion regarding the model and the individual contributions of the TSS, phonons, and bulk electrons to the total thermal conductivity is provided in Supplementary Note 7. The results of one batch of "dead" samples are also shown in Figure 2a, where the thermal conductivities were not tuned by optical gating. Their TSS could be impaired during the sample preparation, as discussed in Supplementary Note 3. The thermal conductivity of these dead samples is close to that of the OFF states of working samples, which is dominated by phonon and bulk electron transport.

Two types of ON/OFF cycling tests were performed together with thermal conductivity measurements. Figure 2b,c presents the power (of the Raman incident laser) dependent Raman peak shift (a measure of temperature) for the 9 nm thick film. One type of test utilized long illumination, which was to place the  $Si_3N_4$  side of the sample directly facing LEDs for a time duration of ~7.5 h, ensuring the  $Si_3N_4$  is fully exposed and the charge sites are saturated. After these long illumination, micro-Raman measurements with ~10 incident Raman laser power levels are conducted, which are shown in Figure 2b,c as solid dots fitted with blue and red lines. The slope of the Raman shift vs the incident power is related to thermal conductivity (smaller slope corresponding to larger thermal conductivity).  $^{53}$  The second cycling test utilized

pulsed illumination, with pulse trains of 1-s-long pulses and a duty cycle of 0.1, i.e., 1 s on, 9 s off. The use of a small duty cycle is to ensure that there is no temperature buildup in the LEDs, hence a consistent dosage throughout the tests, which was verified by monitoring the LED driving current. The illumination time in seconds in Figure 2b-d is the same as the total number of pulses that the samples receive. Hence, the dose of illumination used in optical gating is precisely controlled. During these tests, Raman measurements were performed between the pulse trains using only three different powers (instead of ten) so that the experimental results could be obtained within a shorter time. These Raman shift data for both UV and red pulse illumination are also shown in Figure 2b,c as hollow diamonds, and the sequences are indicated by red and violet arrows, respectively, to indicate the light source. The pulsed illumination results illustrate a continuous process of optically gating the thermal transistor on or off over tens of seconds. The thermal conductivity of each time step is extracted using the same procedure as described above, and the results are plotted in Figure 2d.

We define the response time for the thermal transistor as the time needed to switch from 20% to 80%. From Figure 2d, the ON and OFF switching times are found to be 15 and 40 s, respectively. A detailed discussion regarding the scale and difference of switching times is provided in Supplementary Note 5. However, this switching time is not the limit of the thermal transistor. Figure 1d shows that electrical back gating and optical gating can also achieve the same effect. The electrical measurements shown in Figure 1d were performed in a much faster, continuous manner with no time delay between different back gate voltages. Moreover, the intrinsic switching time from electrical gating is of the order of ~1 ns or faster. Therefore, the thermal transistor can respond much faster when electrical gating is used.

Thermal transistors can be repetitively switched on and off. The thermal conductivity of the 9 nm thermal transistor at room temperature was measured through several illumination cycles, as discussed above. Figure 3 is a representation of these cycling tests. The device first experienced long illuminations to obtain the ON/OFF thermal conductivity presented in Figure 2, which is also shown in Figure 3a. Then, the pulsed trains of red and UV light were applied, and Raman measurements were performed after each time step. The thermal conductivity results are shown in Figure 3b,c. Then, the pulsed trains were

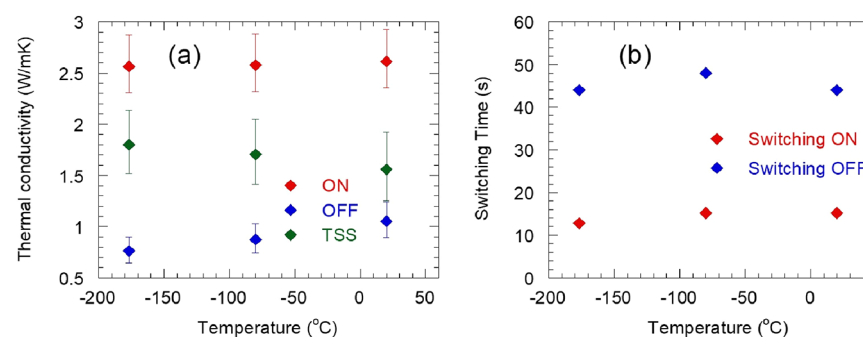


**Figure 4.** Thermal conductivity switching at low temperature. (a) Temperature-dependent thermal conductivity switching of the 9 nm thermal transistor. The TSS contribution is obtained by subtracting the thermal conductivity at the OFF state from that at the ON state. (b) Optical switching time at low temperatures.

used again (with finer time steps), and the results are shown in Figure 2b-d and plotted in Figure 3d,e. A series of low-temperature tests were also performed afterward, and the results are discussed below. After the low-temperature measurements, two more long illumination cycles were performed to verify the repeatability of switching further. It was found that the thermal transistor was able to switch on and off after these (5 room-temperature +2 low-temperature) cycles. Finally, we heat the thermal transistor to 200 °C for 60 min, which is known to damage the TSS due to Se/Te migration. The thermal conductivity of the thermal transistor was measured to be 0.95 W/mK, which is close to that of the dead samples described previously.

We also performed optical gate-dependent thermal conductivity tests at lower temperatures in a liquid nitrogen cryostat. The temperature dependence of the ON/OFF thermal conductivity is shown in Figure 4a. Interestingly, the ON state thermal conductivity, which includes contributions from TSS electrons, bulk electrons, and phonons, does not vary much with temperature, while the OFF state thermal conductivity, which includes contributions from bulk phonons and electrons, decreases with temperature decrease, though only marginally considering the measurement uncertainty. This indicates that the thermal transistor can operate in a wide range, from ~-180 °C to room temperature. Further tests showed that the thermal transistor can be operated up to ~90 °C. From Figure 4a, we observe that the TSS thermal transport increases with decreasing temperature, which indicates that the TSS thermal transport cannot be solely due to bipolar diffusion. This is because bipolar diffusion is thermal energy carried by thermally excited electron-hole pairs, which should be reduced when the temperature is decreased. The possible mechanism that counters the decrease of thermal conductivity with a temperature decrease is the hydrodynamic interaction among electrons, which increases with the temperature decrease.46 It can also be pointed out that the OFF state thermal conductivity is not due to the bipolar diffusion of bulk states because the OFF states are achieved by gating the chemical potential toward the conduction band edge, whereas the bipolar effect exists when chemical potential is within the (small) bandgap. The switching times at low temperatures are found to be similar to the room temperature, i.e.,  $\sim 15$  s for switching on and ~40 s for switching off, as shown in Figure

In summary, we demonstrated the tuning of the thermal conductivity of thin film Bi<sub>2</sub>Te<sub>2</sub>Se by optical gating. The effect of optical gating on sheet resistance is verified by electrostatic

back gating and Hall-effect measurements. The thermal conductivity of thin films can be tuned continuously with a maximum ON/OFF ratio of 2.8 at room temperature within tens of seconds. This switching time can be much improved when using electrical gating. In addition, the thermal transistor can be operated in a wide temperature range from -180 to  $\sim 90\,^{\circ}$ C. Repeated switching over multiple ON/OFF cycles was also demonstrated. This electrostatic thermal transistor with a large ON/OFF ratio and fast switching offers the possibility of smart thermal devices for active thermal management in future electronic devices.

#### ASSOCIATED CONTENT

## Supporting Information

The Supporting Information is available free of charge at https://pubs.acs.org/doi/10.1021/acs.nanolett.3c05085.

(1) Estimation of the effect of back gate; (2) Mechanism of the optical gating effect; (3) Sample preparation and electrical measurements; (4) Hall-effect measurements after red/UV illumination; (5) Details of micro-Raman measurements and optical switching time; (6) Optical gating effect due to Raman laser irradiation; (7) Theoretical model for predicting the TSS contribution to thermal conductivity (PDF)

#### AUTHOR INFORMATION

### **Corresponding Author**

Xianfan Xu — School of Mechanical Engineering, Birck
Nanotechnology Center, and Elmore Family School of
Electrical and Computer Engineering, Purdue University,
West Lafayette, Indiana 47907, United States; ⊚ orcid.org/
0000-0003-0580-4625; Email: xxu@ecn.purdue.edu

#### Authors

Shouyuan Huang – School of Mechanical Engineering and Birck Nanotechnology Center, Purdue University, West Lafayette, Indiana 47907, United States

Neil Ghosh — School of Mechanical Engineering and Birck Nanotechnology Center, Purdue University, West Lafayette, Indiana 47907, United States; orcid.org/0000-0002-0527-011X

Chang Niu — Birck Nanotechnology Center and Elmore Family School of Electrical and Computer Engineering, Purdue University, West Lafayette, Indiana 47907, United States; orcid.org/0000-0003-3175-7164

Yong P. Chen — Birck Nanotechnology Center, Elmore Family School of Electrical and Computer Engineering, Department

of Physics and Astronomy, and Purdue Quantum Science and Engineering Institute, Purdue University, West Lafayette, Indiana 47907, United States

Peide D. Ye — Birck Nanotechnology Center, Elmore Family School of Electrical and Computer Engineering, and Purdue Quantum Science and Engineering Institute, Purdue University, West Lafayette, Indiana 47907, United States; orcid.org/0000-0001-8466-9745

Complete contact information is available at: https://pubs.acs.org/10.1021/acs.nanolett.3c05085

#### **Author Contributions**

¶These authors contributed equally to this work: S.H. and N.G. X.X. conceived the idea and supervised the project. S.H. and N.G. designed the experiments. S.H. performed the thermal conductivity measurements. N.G. and C.N. performed the electrical transport measurements under the supervision of X.X. and P.D.Y. Y.P.C. provided the material. S.H. and N.G. analyzed the experimental data. S.H., N.G., and X.X. cowrote the paper with input from all authors.

#### Notes

The authors declare no competing financial interest.

#### ACKNOWLEDGMENTS

This work was supported in part by the National Science Foundation (CBET-2051525). N.G. acknowledges valuable discussions and technical support from Dr. Rahul Tripathi.

#### REFERENCES

- (1) Wehmeyer, G.; Yabuki, T.; Monachon, C.; Wu, J.; Dames, C. Thermal Diodes, Regulators, and Switches: Physical Mechanisms and Potential Applications. *Applied Physics Reviews* **2017**, *4* (4), No. 041304.
- (2) Swoboda, T.; Klinar, K.; Yalamarthy, A. S.; Kitanovski, A.; Muñoz Rojo, M. Solid-State Thermal Control Devices. *Advanced Electronic Materials* **2021**, *7*, No. 2000625.
- (3) Li, Y.; Li, W.; Han, T.; Zheng, X.; Li, J.; Li, B.; Fan, S.; Qiu, C. W. Transforming Heat Transfer with Thermal Metamaterials and Devices. *Nature Reviews Materials* **2021**, *6* (6), 488–507.
- (4) Sood, A.; Xiong, F.; Chen, S.; Wang, H.; Selli, D.; Zhang, J.; McClellan, C. J.; Sun, J.; Donadio, D.; Cui, Y.; Pop, E.; Goodson, K. E. An Electrochemical Thermal Transistor. *Nat. Commun.* **2018**, *9*, 4510.
- (5) Cho, J.; Richards, C.; Bahr, D.; Jiao, J.; Richards, R. Evaluation of Contacts for a MEMS Thermal Switch. *Journal of Micromechanics and Microengineering* **2008**, *18* (10), No. 105012.
- (6) Klinar, K.; Swoboda, T.; Muñoz Rojo, M.; Kitanovski, A. Fluidic and Mechanical Thermal Control Devices. *Advanced Electronic Materials* **2021**, *7*, No. 2000623.
- (7) Jia, Y.; Ju, Y. S. Solid-Liquid Hybrid Thermal Interfaces for Low-Contact Pressure Thermal Switching. *Journal of Heat Transfer* **2014**, *136*, No. 074503.
- (8) Oh, D. W.; Ko, C.; Ramanathan, S.; Cahill, D. G. Thermal Conductivity and Dynamic Heat Capacity across the Metal-Insulator Transition in Thin Film VO2. *Appl. Phys. Lett.* **2010**, *96* (15), No. 151906.
- (9) Lee, S.; Hippalgaonkar, K.; Yang, F.; Hong, J.; Ko, C.; Suh, J.; Liu, K.; Wang, K.; Urban, J. J.; Zhang, X.; Dames, C.; Hartnoll, S. A.; Delaire, O.; Wu, J. Anomalously Low Electronic Thermal Conductivity in Metallic Vanadium Dioxide. *Science* **2017**, 355 (6323), 371–374.
- (10) Hejtmanek, J.; Jirak, Z.; Marysko, M.; Martin, C.; Maignan, A.; Hervieu, M.; Raveau, B. Interplay between Transport, Magnetic, and Ordering Phenomena in (Formula Presented). *Physical Review B Condensed Matter and Materials Physics* **1999**, *60* (20), 14057–14065.

- (11) Zheng, R.; Gao, J.; Wang, J.; Chen, G. Reversible Temperature Regulation of Electrical and Thermal Conductivity Using Liquid-Solid Phase Transitions. *Nat. Commun.* **2011**, *2*, 289.
- (12) Li, Y.; Dang, Y.; Zhang, S.; Li, X.; Jin, Y.; Ben-Abdallah, P.; Xu, J.; Ma, Y. Radiative Thermal Transistor. *Phys. Rev. Applied* **2023**, *20* (2), No. 024061.
- (13) Li, M.; Wu, H.; Avery, E. M.; Qin, Z.; Goronzy, D. P.; Nguyen, H. D.; Liu, T.; Weiss, P. S.; Hu, Y. Electrically Gated Molecular Thermal Switch. *Science* **2023**, 382 (6670), 585–589.
- (14) Cho, J.; Losego, M. D.; Zhang, H. G.; Kim, H.; Zuo, J.; Petrov, I.; Cahill, D. G.; Braun, P. V. Electrochemically Tunable Thermal Conductivity of Lithium Cobalt Oxide. *Nat. Commun.* **2014**, *5*, 4035.
- (15) Kang, J. S.; Ke, M.; Hu, Y. Ionic Intercalation in Two-Dimensional van Der Waals Materials: In Situ Characterization and Electrochemical Control of the Anisotropic Thermal Conductivity of Black Phosphorus. *Nano Lett.* **2017**, *17* (3), 1431–1438.
- (16) Zhu, G.; Liu, J.; Zheng, Q.; Zhang, R.; Li, D.; Banerjee, D.; Cahill, D. G. Tuning Thermal Conductivity in Molybdenum Disulfide by Electrochemical Intercalation. *Nat. Commun.* **2016**, *7* (1), No. 13211.
- (17) Ishibe, T.; Kaneko, T.; Uematsu, Y.; Sato-Akaba, H.; Komura, M.; Iyoda, T.; Nakamura, Y. Tunable Thermal Switch via Order—Order Transition in Liquid Crystalline Block Copolymer. *Nano Lett.* **2022**, 22 (15), 6105–6111.
- (18) Zhang, Y.; Postiglione, W. M.; Xie, R.; Zhang, C.; Zhou, H.; Chaturvedi, V.; Heltemes, K.; Zhou, H.; Feng, T.; Leighton, C.; Wang, X. Wide-Range Continuous Tuning of the Thermal Conductivity of La0.SSr0.5CoO3- $\delta$  Films via Room-Temperature Ion-Gel Gating. *Nat. Commun.* **2023**, *14* (1), 2626.
- (19) Du, T.; Xiong, Z.; Delgado, L.; Liao, W.; Peoples, J.; Kantharaj, R.; Chowdhury, P. R.; Marconnet, A.; Ruan, X. Wide Range Continuously Tunable and Fast Thermal Switching Based on Compressible Graphene Composite Foams. *Nat. Commun.* **2021**, 12, 4915.
- (20) Ott, A.; Hu, Y.; Wu, X. H.; Biehs, S. A. Radiative Thermal Switch Exploiting Hyperbolic Surface Phonon Polaritons. *Physical Review Applied* **2021**, *15*, No. 064073.
- (21) Ihlefeld, J. F.; Foley, B. M.; Scrymgeour, D. A.; Michael, J. R.; McKenzie, B. B.; Medlin, D. L.; Wallace, M.; Trolier-Mckinstry, S.; Hopkins, P. E. Room-Temperature Voltage Tunable Phonon Thermal Conductivity via Reconfigurable Interfaces in Ferroelectric Thin Films. *Nano Lett.* **2015**, *15* (3), 1791–1795.
- (22) Aryana, K.; Tomko, J. A.; Gao, R.; Hoglund, E. R.; Mimura, T.; Makarem, S.; Salanova, A.; Hoque, M. S. B.; Pfeifer, T. W.; Olson, D. H.; Braun, J. L.; Nag, J.; Read, J. C.; Howe, J. M.; Opila, E. J.; Martin, L. W.; Ihlefeld, J. F.; Hopkins, P. E. Observation of Solid-State Bidirectional Thermal Conductivity Switching in Antiferroelectric Lead Zirconate (PbZrO3). *Nat. Commun.* 2022, *13*, 1573.
- (23) Yang, Y.; Zhu, J. G.; White, R. M.; Asheghi, M. Field-Dependent Thermal and Electrical Transports in Cu/CoFe Multilayer. *J. Appl. Phys.* **2006**, *99*, No. 063703.
- (24) Kimling, J.; Nielsch, K.; Rott, K.; Reiss, G. Field-Dependent Thermal Conductivity and Lorenz Number in Co/Cu Multilayers. *Physical Review B Condensed Matter and Materials Physics* **2013**, 87, No. 134406.
- (25) Kimling, J.; Wilson, R. B.; Rott, K.; Kimling, J.; Reiss, G.; Cahill, D. G. Spin-Dependent Thermal Transport Perpendicular to the Planes of Co/Cu Multilayers. *Physical Review B Condensed Matter and Materials Physics* **2015**, 91, No. 144405.
- (26) Shin, J.; Kang, M.; Tsai, T.; Leal, C.; Braun, P. V.; Cahill, D. G. Thermally Functional Liquid Crystal Networks by Magnetic Field Driven Molecular Orientation. *ACS Macro Lett.* **2016**, *5* (8), 955–960.
- (27) Shen, T. Z.; Hong, S. H.; Song, J. K. Electro-Optical Switching of Graphene Oxide Liquid Crystals with an Extremely Large Kerr Coefficient. *Nat. Mater.* **2014**, *13* (4), 394–399.
- (28) Lin, F.; Zhu, Z.; Zhou, X.; Qiu, W.; Niu, C.; Hu, J.; Dahal, K.; Wang, Y.; Zhao, Z.; Ren, Z.; Litvinov, D.; Liu, Z.; Wang, Z. M.; Bao, J. Orientation Control of Graphene Flakes by Magnetic Field: Broad

- Device Applications of Macroscopically Aligned Graphene. *Adv. Mater.* **2017**, 29, No. 1604453.
- (29) Wu, Y.; Li, D.; Wu, C.-L.; Hwang, H. Y.; Cui, Y. Electrostatic Gating and Intercalation in 2D Materials. *Nat. Rev. Mater.* **2023**, 8 (1), 41–53.
- (30) Ghosh, S.; Calizo, I.; Teweldebrhan, D.; Pokatilov, E. P.; Nika, D. L.; Balandin, A. A.; Bao, W.; Miao, F.; Lau, C. N. Extremely High Thermal Conductivity of Graphene: Prospects for Thermal Management Applications in Nanoelectronic Circuits. *Appl. Phys. Lett.* **2008**, 92 (15), No. 151911.
- (31) Nika, D. L.; Pokatilov, E. P.; Askerov, A. S.; Balandin, A. A. Phonon Thermal Conduction in Graphene: Role of Umklapp and Edge Roughness Scattering. *Phys. Rev. B* **2009**, *79* (15), No. 155413.
- (32) Sagmeister, M.; Brossmann, U.; Landgraf, S.; Würschum, R. Electrically Tunable Resistance of a Metal. *Phys. Rev. Lett.* **2006**, *96* (15), No. 156601.
- (33) Breunig, O.; Ando, Y. Opportunities in Topological Insulator Devices. *Nat. Rev. Phys.* **2022**, *4* (3), 184–193.
- (34) Politano, A.; Viti, L.; Vitiello, M. S. Optoelectronic Devices, Plasmonics, and Photonics with Topological Insulators. *APL Materials* **2017**, *5* (3), No. 035504.
- (35) Dang, L. T.; Breunig, O.; Wang, Z.; Legg, H. F.; Ando, Y. Topological-Insulator Spin Transistor. *Phys. Rev. Applied* **2023**, 20 (2), No. 024065.
- (36) Hu, G.; Zhang, Y.; Li, L.; Wang, Z. L. Piezotronic Transistor Based on Topological Insulators. ACS Nano 2018, 12 (1), 779–785.
- (37) Huang, S.; Xu, X. Optical Chirality Detection Using a Topological Insulator Transistor. *Adv. Optical Mater.* **2021**, 9 (10), No. 2002210.
- (38) Huang, S.; Miotkowski, I.; Chen, Y. P.; Xu, X. Deep Tuning of Photo-Thermoelectricity in Topological Surface States. *Sci. Rep.* **2020**, *10* (1), 16761.
- (39) McIver, J. W.; Hsieh, D.; Steinberg, H.; Jarillo-Herrero, P.; Gedik, N. Control over Topological Insulator Photocurrents with Light Polarization. *Nat. Nanotechnol.* **2012**, *7* (2), 96–100.
- (40) Niu, C.; Huang, S.; Ghosh, N.; Tan, P.; Wang, M.; Wu, W.; Xu, X.; Ye, P. D. Tunable Circular Photogalvanic and Photovoltaic Effect in 2D Tellurium with Different Chirality. *Nano Lett.* **2023**, 23, 3599.
- (41) Qiu, G.; Niu, C.; Wang, Y.; Si, M.; Zhang, Z.; Wu, W.; Ye, P. D. Quantum Hall Effect of Weyl Fermions in N-Type Semiconducting Tellurene. *Nat. Nanotechnol.* **2020**, *15* (7), 585–591.
- (42) Hirayama, M.; Okugawa, R.; Ishibashi, S.; Murakami, S.; Miyake, T. Weyl Node and Spin Texture in Trigonal Tellurium and Selenium. *Phys. Rev. Lett.* **2015**, *114* (20), No. 206401.
- (43) Tian, J.; Miotkowski, I.; Hong, S.; Chen, Y. P. Electrical Injection and Detection of Spin-Polarized Currents in Topological Insulator Bi2Te2Se. *Sci. Rep.* **2015**, *5*, No. 14293.
- (44) Tian, J.; Hong, S.; Miotkowski, I.; Datta, S.; Chen, Y. P. Observation of Current-Induced, Long-Lived Persistent Spin Polarization in a Topological Insulator: A Rechargeable Spin Battery. *Sci. Adv.* **2017**, 3 (4), No. e1602531.
- (45) Luo, Z.; Tian, J.; Huang, S.; Srinivasan, M.; Maassen, J.; Chen, Y. P.; Xu, X. Large Enhancement of Thermal Conductivity and Lorenz Number in Topological Insulator Thin Films. *ACS Nano* **2018**, *12* (2), 1120–1127.
- (46) Crossno, J.; Shi, J. K.; Wang, K.; Liu, X.; Harzheim, A.; Lucas, A.; Sachdev, S.; Kim, P.; Taniguchi, T.; Watanabe, K.; Ohki, T. A.; Fong, K. C. Observation of the Dirac Fluid and the Breakdown of the Wiedemann-Franz Law in Graphene. *Science* **2016**, *351* (6277), 1058–1061.
- (47) Liu, F.; Zhu, C.; You, L.; Liang, S.; Zheng, S.; Zhou, J.; Fu, Q.; He, Y.; Zeng, Q.; Fan, H. J.; Ang, L. K.; Wang, J.; Liu, Z. 2D Black Phosphorus/SrTiO <sub>3</sub> -Based Programmable Photoconductive Switch. *Adv. Mater.* **2016**, 28 (35), 7768–7773.
- (48) Ho, P.-H.; Shih, Y.-S.; Li, M.-K.; Chen, T.-P.; Shih, F.-Y.; Wang, W.-H.; Chen, C.-W. Spatially and Precisely Controlled Large-Scale and Persistent Optical Gating in a TiO <sub>x</sub> MoS <sub>2</sub> Heterostructure. *ACS Appl. Mater. Interfaces* **2018**, *10* (44), 38319–38325.

- (49) Yang, M.; Yan, C.; Ma, Y.; Li, L.; Cen, C. Light Induced Non-Volatile Switching of Superconductivity in Single Layer FeSe on SrTiO3 Substrate. *Nat. Commun.* **2019**, *10* (1), 85.
- (50) Yeats, A. L.; Pan, Y.; Richardella, A.; Mintun, P. J.; Samarth, N.; Awschalom, D. D. Persistent Optical Gating of a Topological Insulator. *Sci. Adv.* **2015**, *1* (9), No. e150064.
- (51) Liu, T.; Xiang, D.; Zheng, Y.; Wang, Y.; Wang, X.; Wang, L.; He, J.; Liu, L.; Chen, W. Nonvolatile and Programmable Photodoping in MoTe <sub>2</sub> for Photoresist-Free Complementary Electronic Devices. *Adv. Mater.* **2018**, *30* (52), No. 1804470.
- (52) Robertson, J. Band Offsets of Wide-Band-Gap Oxides and Implications for Future Electronic Devices. *Journal of Vacuum Science & Technology B: Microelectronics and Nanometer Structures Processing, Measurement, and Phenomena* **2000**, 18 (3), 1785–1791.
- (53) Luo, Z.; Liu, H.; Spann, B. T.; Feng, Y.; Ye, P.; Chen, Y. P.; Xu, X. Measurement of In-Plane Thermal Conductivity of Ultrathin Films Using Micro-Raman Spectroscopy. *Nanoscale and Microscale Thermophysical Engineering* **2014**, *18* (2), 183–193.
- (54) Balandin, A. A.; Ghosh, S.; Bao, W.; Calizo, I.; Teweldebrhan, D.; Miao, F.; Lau, C. N. Superior Thermal Conductivity of Single-Layer Graphene. *Nano Lett.* **2008**, *8* (3), 902–907.
- (55) Cai, W.; Moore, A. L.; Zhu, Y.; Li, X.; Chen, S.; Shi, L.; Ruoff, R. S. Thermal Transport in Suspended and Supported Monolayer Graphene Grown by Chemical Vapor Deposition. *Nano Lett.* **2010**, *10* (5), 1645–1651.
- (56) Yan, R.; Simpson, J. R.; Bertolazzi, S.; Brivio, J.; Watson, M.; Wu, X.; Kis, A.; Luo, T.; Hight Walker, A. R.; Xing, H. G. Thermal Conductivity of Monolayer Molybdenum Disulfide Obtained from Temperature-Dependent Raman Spectroscopy. *ACS Nano* **2014**, 8 (1), 986–993.
- (57) Zhou, H.; Zhu, J.; Liu, Z.; Yan, Z.; Fan, X.; Lin, J.; Wang, G.; Yan, Q.; Yu, T.; Ajayan, P. M.; Tour, J. M. High Thermal Conductivity of Suspended Few-Layer Hexagonal Boron Nitride Sheets. *Nano Research* **2014**, *7* (8), 1232–1240.
- (58) Luo, Z.; Maassen, J.; Deng, Y.; Du, Y.; Garrelts, R. P.; Lundstrom, M. S; Ye, P. D.; Xu, X. Anisotropic In-Plane Thermal Conductivity Observed in Few-Layer Black Phosphorus. *Nat. Commun.* **2015**, *6*, 8572.
- (59) Peimyoo, N.; Shang, J.; Yang, W.; Wang, Y.; Cong, C.; Yu, T. Thermal Conductivity Determination of Suspended Mono- and Bilayer WS2 by Raman Spectroscopy. *Nano Research* **2015**, *8* (4), 1210–1221.
- (60) Wang, R.; Wang, T.; Zobeiri, H.; Yuan, P.; Deng, C.; Yue, Y.; Xu, S.; Wang, X. Measurement of the Thermal Conductivities of Suspended MoS<sub>2</sub> and MoSe<sub>2</sub> by Nanosecond ET-Raman without Temperature Calibration and Laser Absorption Evaluation. *Nanoscale* **2018**, *10* (48), 23087–23102.
- (61) Xu, S.; Fan, A.; Wang, H.; Zhang, X.; Wang, X. Raman-Based Nanoscale Thermal Transport Characterization: A Critical Review. *Int. J. Heat Mass Transfer* **2020**, *154*, No. 119751.
- (62) Huang, S.; Chen, Y.; Luo, Z.; Xu, X. Temperature and Strain Effects in Micro-Raman Thermometry for Measuring In-Plane Thermal Conductivity of Thin Films. *Nanoscale and Microscale Thermophysical Engineering* **2021**, 25 (2), 91–100.
- (63) Luo, Z.; Tian, J.; Huang, S.; Srinivasan, M.; Maassen, J.; Chen, Y. P.; Xu, X. Large Enhancement of Thermal Conductivity and Lorenz Number in Topological Insulator Thin Films. *ACS Nano* **2018**, *12* (2), 1120–1127.
- (64) Seifert, P.; Vaklinova, K.; Kern, K.; Burghard, M.; Holleitner, A. Surface State-Dominated Photoconduction and THz Generation in Topological Bi2Te2Se Nanowires. *Nano Lett.* **2017**, *17*, 973–979.
- (65) Bahramy, M. S.; King, P. D. C.; De La Torre, A.; Chang, J.; Shi, M.; Patthey, L.; Balakrishnan, G.; Hofmann, P.; Arita, R.; Nagaosa, N.; Baumberger, F. Emergent Quantum Confinement at Topological Insulator Surfaces. *Nat. Commun.* **2012**, *3*, 1159.